THE JOURNAL OF PHYSICAL CHEMISTRY B LETTERS

2006, *110,* 6428−6431
Published on Web 03/10/2006

Vibrational Spectra of Methane Clathrate Hydrates from Molecular Dynamics Simulation

Jeffery A. Greathouse* and Randall T. Cygan

Sandia National Laboratories, Albuquerque, New Mexico 87185-0754

Blake A. Simmons

Sandia National Laboratories, Livermore, California 94551-0969

Received: January 23, 2006; In Final Form: February 24, 2006

Molecular dynamics simulations were performed on methane clathrate hydrates at ambient conditions. Thermal expansion results over the temperature range 60−300 K show that the unit cell volume increases with temperature in agreement with experiment. Power spectra were obtained at 273 K from velocity autocorrelation functions for selected atoms, and normal modes were assigned. The spectra were further classified according to individual atom types, allowing the assignment of contributions from methane molecules located in small and large cages within the structure I unit cell. The symmetric C−H stretch of methane in the small cages occurs at a higher frequency than for methane located in the large cages, with a peak separation of 14 cm^{-1}. Additionally, we determined that the symmetric C−H stretch in methane gas occurs at the same frequency as methane in the large cages. Results of molecular dynamics simulations indicate the use of power spectra obtained from the velocity autocorrelation function is a reliable method to investigate the vibrational behavior of guest molecules in clathrate hydrates.

Introduction

Clathrate hydrates are characterized by the general formula $X{\cdot}nH_2O$, where X is the guest molecule within a water cage, and *n* is the hydration number per guest molecule. Hydrates that form with a gas-phase guest molecule are termed gas hydrates and have been the focus of experimental and theoretical study in recent decades.[1] In particular, methane hydrates have received much attention in the literature due to their abundance in nature and as a potential future energy source.[2] The unit cell for the common methane hydrate, termed structure I,[1] consists of two small cages and six large cages. The two cages consist of 20 and 24 water molecules, respectively. The molecular diameter of methane allows it to occupy both cages, with an average hydration number of approximately six.[3]

More recently, computational methods have been used to study gas hydrates.[4−13] Once again, methane hydrates receive the most attention, and the goal of these projects has been to validate the published experimental data on thermodynamics of hydrate formation.[5−13] Most molecular simulation studies to date have focused on simple energy force fields, treating water molecules as rigid bodies and methane molecules as spherical particles. In one study, structural properties of methane hydrates were compared using a variety of rigid water models (polarizable and nonpolarizable) and one flexible water model.[5] The average water dipole moment using the rigid polarizable model was considerably larger than the other water models, and the radial distribution functions showed a more ordered structure using the rigid polarizable model.[5] Similar simulations have also been used to compare the thermodynamics of cage occupancies with predictions from statistical thermodynamics.[4,9,13]

Use of such simple force fields may be sufficient for studies of phase behavior or thermodynamic properties, but not for molecular detail such as vibrational modes. Vibrational spectroscopy, and in particular Raman spectroscopy, of guest molecules in gas hydrates can be a useful tool in determining many aspects of guest−host relationships, including identification of the guest species, hydration number of the guest molecules, and their occupancies.[1] Two recent Raman spectroscopic studies of methane hydrates have attempted to quantify the occupancy of methane molecules in both cage types.[14,15] The symmetric C−H stretching mode was split into two peaks (≈2905 cm^{-1} and ≈2915 cm^{-1})[14,15] compared to the single peak at 2917 cm^{-1} in the spectrum of methane gas.[16] The assignment of the large cage at 2905 cm^{-1} and the small cage at 2915 cm^{-1} (coincident with the methane gas peak) was based on peak intensitiess[14] but seems counterintuitive considering that a methane molecule in a large cage has more translational freedom of motion (like methane gas) than methane in a small cage. In a previous study, these peak assignments were reversed so that the higher frequency peak (2915 cm^{-1}) was assigned to methane in the large cage.[17]

Molecular simulations, specifically molecular dynamics methods, can also be used to provide vibrational frequencies in the form of a power spectrum.[18] Provided that molecular flexibility in the form of bond stretching and angle bending terms are included in the force field energy expression, dynamics trajectories can be analyzed and spectra can be calculated. In this study we computed the vibrational spectra for selected atoms, allowing spectral peak contributions from methane molecules located in large and small cages to be unambiguously assigned. Our work presented here is similar to that of a previous simulation study of methane hydrates.[19] However, none of the

* To whom correspondence should be addressed: jagreat@sandia.gov.

10.1021/jp060471t CCC: $33.50

calculated frequencies in this previous work were within 50 cm^{-1} of the Raman spectrum of pure methane.[19] This is especially surprising for the bend and rocking modes of methane. The simulations were performed at 100 K, although the experimental Raman spectra were collected near 273 K.[14,15] Finally, the simulations were performed for 4 ps following an equilibration period of only 4 ps, and data were not shown to indicate that the systems were equilibrated.[19]

Methods

The consistent valence force field (CVFF)[20] was used for all intermolecular and intramolecular interactions. CVFF uses a flexible version of the simple point charge (SPC) water model,[21] which has atomic charges of +0.41 *e* and −0.82 *e* for H and O atoms, respectively. Charges for methane atoms (+0.1 *e* for H, −0.4 *e* for C) were determined from a bond increment technique within CVFF.[20] Intermolecular interactions consisted of electrostatic and Lennard-Jones 6−12 terms, while intramolecular interactions included bond stretch and angle bend terms. Other methane potentials have been derived specifically for methane hydrate simulations,[22−24] but as mentioned above they treat the methane molecule as a rigid body. The lowest nonzero multipole moment for methane is the octupole moment, which for the CVFF methane molecule is less than the experimental value.[23] Since we are interested in intramolecular interactions, we must use a model that incorporates bond stretch and angle bend terms. Therefore, the octupole moment of methane is actually a dynamic quantity when a flexible force field like CVFF is used. We hope to show that the use of CVFF for a wide variety organic guest molecules results in realistic models of gas hydrates from structural, thermodynamic, and dynamic considerations.

The initial placement of water oxygen atoms was taken from neutron diffraction coordinates of ethylene oxide deuteriohydrate,[25] and the supercell contained 8 unit cells of clathrate in a 2×2×2 expansion. The simulation cell contained 48 large cages and 16 small cages, with an initial cell length of 23.74 Å. All cages were filled with one methane molecule, and a carbon atom was placed at the center of each cage. Hydrogen atoms were added to each molecule, and their initial positions were determined by a series of energy minimizations with fixed carbon and oxygen positions. This procedure produces a reasonable hydrogen bonded network of water molecules suitable for further simulation. A series of *NVT* (number of atoms, volume, temperature) simulations were used to equilibrate the system before a final *NPT* (P = pressure, 1.5 ps relaxation time) simulation for 1.0 ns was performed. The thermostat relaxation time was 0.1 ps for all simulations. During the *NPT* simulation, cell angles were fixed at 90°, but each cell length was allowed to vary independently. These simulations were carried out with $P = 0$ atm and temperatures of 60, 100, 150, 200, 250, 273, and 300 K.

Simulations were also performed on methane gas at low (34 bar) and high (300 bar) pressures and a temperature of 273 K. Pressures were determined based on the ideal gas equation with the following molecular dynamics supercell configurations: 34 bar (27 molecules, 31.17 Å cell length) and 300 bar (64 molecules, 20.0 Å cell length). All simulations of methane gas were conducted in the *NVT* ensemble with $T = 273$ K to provide an accurate comparison of power spectra between methane gas and methane hydrate, and to match as closely as possible the temperature conditions of the Raman experiments.[14,15] All molecular dynamics simulations discussed above were carried out with the LAMMPS code.[26] Short-range potential energy terms (10.0 Å cutoff) were evaluated every 0.0005 ps, and long-range electrostatic terms were evaluated every 0.001 ps using an efficient particle−particle particle-mesh solver.[27]

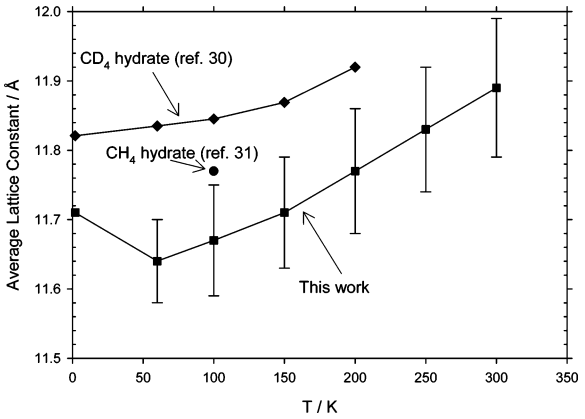

Figure 1. Average lattice parameters for methane hydrate as a function of temperature. Experimental values (errors less than 0.01 Å) obtained from neutron diffraction are also shown for CD_4 hydrate[30] and CH_4 hydrate.[31]

A separate set of *NVT* simulations at 273 K were subsequently performed and analyzed using the OFF dynamics module of Cerius[2] (Accelrys Inc., San Diego) with simulation parameters discussed previously.[28] The initial configurations were taken from previously equilibrated *NPT* snapshots in which the cell lengths were within 0.01 Å of their equilibrium values. For the Cerius[2] simulations, all energy contributions were calculated every 0.0005 ps and real-space energy terms were evaluated with a spline cutoff distance of 8.5 Å. Following an initial stage of 20.0 ps, atomic velocities were stored every 8 steps (0.004 ps) during a production stage of 40.0 ps. This combination of simulation time and storage frequency has been used to produce power spectra of organic condensed phases.[29] The velocity autocorrelation function (VACF)[18] was calculated for each dynamics simulation from the stored atomic velocities. For the VACF calculation, functions were calculated over a 20.0 fs period and then averaged. Separate VACF calculations were performed on individual atom types or combinations of atom types (e.g., methane atoms in small cages, methane atoms in large cages). Power spectra were then calculated by applying a Fourier transform to each VACF with a frequency interval (resolution) of 1 cm^{-1}. English and MacElroy have shown that VACFs of methane hydrates are identical in either the *NVE* (E = potential energy)[5] or *NVT* ensembles, so we are justified in using the *NVT* ensemble in this work.

Results

Structural information obtained from the *NPT* simulations were compared with available neutron diffraction results.[30,31] Figure 1a shows the simulated thermal expansion trend of the lattice parameters from 0 to 300 K. The data point at 0 K was obtained by performing an energy minimization using the Cerius[2] OFF minimizer while allowing the cell volume to vary. Because the supercell dimensions (x, y, z) were allowed to vary independently of each other during the molecular dynamics run, each dimension was recorded separately. A range of unit cell lengths was also seen in simulations of H_2-clathrates.[4] The y-dimension was consistently larger than x or z by 0.05 Å − 0.08 Å at each temperature (data not shown). The unequal lattice parameters were likely due to a net dipole of the supercell, caused by the disordered orientation of water hydrogen atoms.[4] This effect is the result of using a finite supercell with periodic

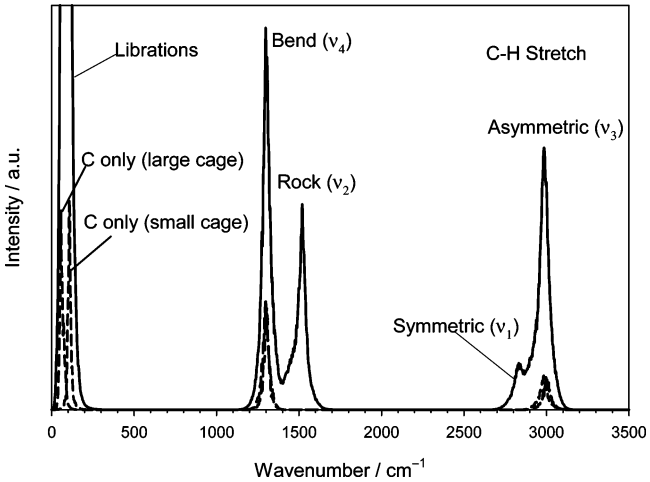

Figure 2. Simulated power spectra of methane atoms in methane hydrate. The solid line represents methane H atoms, and the dashed lines represent methane C atoms in large and small cages. The C atom peaks at 1300 cm^{-1} and 3000 cm^{-1} were multiplied by a factor of 50 for ease of viewing. Contributions from water molecules are not shown for clarity.

TABLE 1: Vibrational Peak Assignments for Methane[a]

phase	method	bend (ν_4)	rock (ν_2)	symmetric stretch (ν_1)	asymmetric stretch (ν_3)
hydrate	this work	1304	1520	2826 (large) 2842 (small)	2986 (large) 3000 (small)
	simulation[19]	1255	1395	2990 (large) 3000 (small)	3075 (large) 3085 (small)
	Raman[14]			2905 (large) 2915 (small)	
gas	this work	1297	1524	2827	2976
	ab initio[32]	1345	1570	3036	3157
	Raman[16]	1306	1535	2917	3020
liquid	simulation[19]	1242	1410	2975	3067

[a] Comparisons are made with ab initio calculations and the experimental Raman spectrum of methane gas. All frequencies are in cm^{-1}.

boundary conditions and would not be seen experimentally. All simulations began with the same initial coordinates, which is the likely explanation for the consistent appearance of *y* as the expanded dimension. The results in Figure 1 were obtained by averaging the *x*, *y*, and *z* values at each frame. The simulation results are in qualitative agreement with the neutron diffraction data of CD_4 hydrates,[30,31] but the lattice parameters are shifted to smaller values by approximately 0.15 Å at each temperature. The fact that the experimental lattice parameters for CD_4 and CH_4 hydrates at 100 K disagree by 0.08 Å suggests that there is some variability in those results as well. Additionally, the CD_4 hydrate patterns also contained signals for hexagonal ice Ih and solid N_2.[30] Overall we find excellent agreement between the simulated and experimental lattice constants over the temperature range 60−200 K.

Separate *NVT* simulations were performed using Cerius[2] OFF dynamics in order to obtain VACF data. The vibrational and librational spectra of methane molecules in both the gas (300 bar) and hydrate phases were obtained from the Fourier transform of the VACFs. Power spectra of the methane hydrogen atoms at 273 K are shown in Figure 2. The four vibrational modes are easily seen, but the assignment of normal modes required a separate calculation of only C atoms. Only the bending and asymmetric C−H stretch modes should involve motion of the C atoms. The frequency assignments are given in Table 1 and compared with those from the methane gas simulation. Our calculated frequencies for the bending and

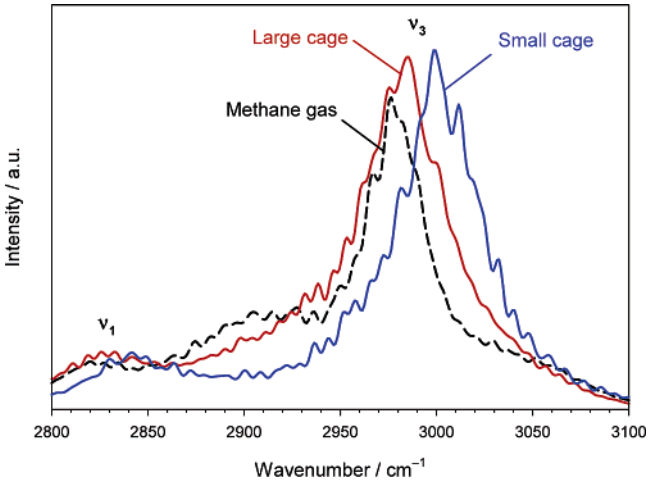

Figure 3. Simulated power spectra of methane H atoms in hydrate (solid lines) and gas (dashed line) phases, focusing on the C−H stretch region.

rocking modes are in excellent agreement with Raman spectra.[16] The poor agreement in the stretching modes is most likely related to the bond stretch (Morse function) potential used in CVFF.[20] The gas-phase ab initio results[32] are in poor agreement with experiment for all normal modes.

An advantage of force-field-based molecular simulations is that methane molecules in large and small cages can be differentiated (dashed lines in Figure 2). The librational motion of methane molecules in small cages occurs at higher frequency (102 cm^{-1}) than methane molecules in the large cages (61 cm^{-1}) due to the reduced free volume in the small cage. The C−H stretching modes can also be used to distinguish between methane in small and large cages, as seen in Figure 3. Peaks for the small and large cages are separated by 14 cm^{-1}, which is in agreement with a splitting of approximately 10 cm^{-1} seen in the Raman spectra.[14,15] Figure 3 also shows that the stretching modes of methane gas are coincident with molecules located in large cages. The spectrum of methane gas at 34 bar is similar to that at 300 bar, but the statistics are poor due to the small number of molecules in the simulation cell. The correlation between local environment of methane and vibrational frequency is intuitive based on nearest-neighbor considerations, indicating that methane molecules in the small cages are in a perturbed state compared to methane gas. Our results are in qualitative agreement with previous simulation results, which also showed both C−H stretching modes for methane molecules located in large cages occurring at a lower frequency than for methane molecules located in small cages.[19] In two previous Raman studies of methane hydrates, the high-frequency peak (2915 cm^{-1}) was coincident with that of methane gas at 34 bar.[14,15] This peak was designated as the contribution from small cages based on peak intensity considerations and associated predictions of cage occupancies.[14,15] The Raman peak assignments are also supported by NMR and other experiments that yield cage occupancies. In light of our results, it might be worth considering that the experimental peak at 2915 cm^{-1} is due to methane molecules in large cages, not small cages. Some doubt could be cast on the simulation results because, unlike the Raman results, the gas-phase peak is coincident with the lower frequency peak. However, our simulations demonstrate that the vibrational behavior of methane molecules occupying large cages is similar to that of methane gas.

Despite the simple nature of classical force fields in describing intramolecular energy associated with bond stretch and angle bend motions, the resulting power spectra can be very useful

in elucidating molecular behavior. We intend to apply this computational technique in the analysis of more complex structure II hydrates and other guest molecules.

Acknowledgment. We would like to thank R. W. Bradshaw and E. H. Majzoub for helpful discussions and J. Clawson for reviewing the manuscript. We acknowledge support from the Sandia National Laboratories under its LDRD program. Sandia is a multiprogram laboratory operated by Sandia Corporation, a Lockheed Martin Company, for the United States Department of Energy's National Nuclear Security Administration under Contract DE-AC04-94AL85000.

References and Notes

(1) Sloan, E. D., Jr. *Clathrate Hydrates of Natural Gases*; Marcel Dekker: New York, 1998.
(2) Buffett, B. A. *Annu. Rev. Earth Planet. Sci.* **2000**, *28*, 477.
(3) Ripmeester, J. A.; Ratcliffe, C. I. *J. Phys. Chem.* **1988**, *92*, 337.
(4) Alavi, S.; Ripmeester, J. A.; Klug, D. D. *J. Chem. Phys.* **2005**, *123*, 024507.
(5) English, N. J.; MacElroy, J. M. D. *J. Comput. Chem.* **2003**, *24*, 1569.
(6) Moon, C.; Taylor, P. C.; Rodger, P. M. *J. Am. Chem. Soc.* **2003**, *125*, 4706.
(7) Storr, M. T.; Taylor, P. C.; Monfort, J. P.; Rodger, P. M. *J. Am. Chem. Soc.* **2004**, *126*, 1569.
(8) Chialvo, A. A.; Houssa, M.; Cummings, P. T. *J. Phys. Chem. B* **2002**, *106*, 442.
(9) Cao, Z. T.; Tester, J. W.; Sparks, K. A.; Trout, B. L. *J. Phys. Chem. B* **2001**, *105*, 10950.
(10) Zele, S. R.; Lee, S.-Y.; Holder, G. D. *J. Phys. Chem. B* **1999**, *103*, 10250.
(11) Forrisddahl, O. K.; Kvamme, B.; Haymet, A. D. J. *Mol. Phys.* **1996**, *89*, 819.
(12) Klauda, J. B.; Sandler, S. I. *Chem. Eng. Sci.* **2003**, *58*, 27.
(13) Klauda, J. B.; Sandler, S. I. *J. Phys. Chem. B* **2002**, *106*, 5722.
(14) Sum, A. K.; Burruss, R. C.; Sloan, E. D. *J. Phys. Chem. B* **1997**, *101*, 7371.
(15) Uchida, T.; Hirano, T.; Ebinuma, T.; Narita, H.; Gohara, K.; Mae, S.; Matsumoto, R. *AIChE J.* **1999**, *45*, 2641.
(16) Schrotter, H. W.; Klockner, H. W. Raman Scattering Cross Sections in Gases and Liquids. In *Raman Spectroscopy of Gases and Liquids*; Weber, A., Ed.; Springer-Verlag: Berlin, 1979; Vol. 11; p 123.
(17) Seitz, J. C.; Pasteris, J. D.; Wopenka, B. *Geochim. Cosmochim. Acta* **1987**, *51*, 1651.
(18) Frenkel, D.; Smit, B. *Understanding Molecular Simulation: From Algorithms to Applications*, 2nd ed.; Academic Press: San Diego, 2002.
(19) Itoh, H.; Kawamura, K. *Ann. N. Y. Acad. Sci.* **2000**, *912*, 693.
(20) Dauber-Osguthorpe, P.; Roberts, V. A.; Osguthorpe, D. J.; Wolff, J.; Genest, M.; Hagler, A. T. *Proteins: Struct., Funct., Genet.* **1988**, *4*, 31.
(21) Teleman, O.; Jonsson, B.; Engstrom, S. *Mol. Phys.* **1987**, *60*, 193.
(22) Anderson, B. J.; Tester, J. W.; Trout, B. L. *J. Phys. Chem. B* **2004**, *108*, 18705.
(23) Righini, R.; Maki, K.; Klein, M. L. *Chem. Phys. Lett.* **1981**, *80*, 301.
(24) Murad, S.; Gubbins, K. E. Molecular Dynamics Simulation of Methane Using a Singularity-free Algorithm. In *Computer Modeling of Matter*; Lykos, P., Ed.; American Chemical Society: Washington, D. C., 1978; p 62.
(25) Hollander, F.; Jeffrey, G. A. *J. Chem. Phys.* **1977**, *66*, 4699.
(26) Plimpton, S. J. *J. Comput. Phys.* **1995**, *117*, 1.
(27) Plimpton, S. J.; Pollock, R.; Stevens, M. "Particle-Mesh Ewald and rRESPA for Parallel Molecular Dynamics Simulations"; Eighth SIAM Conference on Parallel Processing for Scientific Computing, 1997.
(28) Cygan, R. T.; Guggenheim, S.; van Groos, A. F. K. *J. Phys. Chem. B* **2004**, *108*, 15141.
(29) Li, Y.; Lin, S.-T.; Goddard, W. A., III *J. Am. Chem. Soc.* **2004**, *126*, 1872.
(30) Gutt, G.; Asmussen, B.; Press, W.; Johnson, M. R.; Handa, Y. P.; Tse, J. S. *J. Chem. Phys.* **2000**, *113*, 4713.
(31) Davidson, D. W.; Handa, Y. P.; Ratcliffe, C. I.; Tse, J. S.; Powell, B. M. *Nature* **1984**, *311*, 142.
(32) Lee, T. J.; Martin, P. R.; Taylor, J. *J. Chem. Phys.* **1995**, *102*, 254.